



Mass transfer analysis and kinetic modeling for process design of countercurrent membrane supported reactive extraction of carboxylic acids



Angelo Gössi^{a,b}, Wolfgang Riedl^b, Boelo Schuur^{a,*}

^a University of Twente, Faculty of Science and Technology, Sustainable Process Technology Group, 7500AE Enschede, the Netherlands

^b University of Applied Sciences and Arts Northwestern Switzerland, Institute for Chemistry and Bioanalytics, Hofackerstrasse 30, 4132 Muttenz, Switzerland

ARTICLE INFO

Article history:

Received 31 May 2021

Received in revised form 12 September 2021

Accepted 1 November 2021

Keywords:

Reactive extraction

Product recovery

Carboxylic acid

Membrane extraction

ABSTRACT

Countercurrent membrane supported reactive extraction (MSRE) was studied for removal of carboxylic acids from aqueous streams with a PTFE capillary membrane. Analysis of the mass transfer rates was performed to support modeling of the process. Total mass transfer coefficients ranging from $2.0 \cdot 10^{-7}$ to $4.0 \cdot 10^{-7}$ m/s were obtained when extracting lactic acid with 20 wt% tri-N-octyl amine in 1-decanol with membrane thicknesses of 260 μm and 80 μm . The limiting mass transfer resistance in all experiments was in the membrane phase. The developed model based on mass transfer and reaction in parallel allows to predict countercurrent extraction. Experimental validation with 5, 7 and 12 m long membrane modules showed excellent accordance for two acids, validating the model simulations. Simulated membrane contactor lengths required for single, two and three countercurrent stages varied between 10 and 39 m/stage for lactic, mandelic, succinic, itaconic and citric acid, depending on acid, membrane, and diluent.

© 2021 The Authors. Published by Elsevier Ltd. This is an open access article under the CC BY license (<http://creativecommons.org/licenses/by/4.0/>).

1. Introduction

The demand for bio-based chemicals has increased extraordinarily in the last few years, and particularly bio-based polymers are highly desired (Kuznetsov et al., 2017). Carboxylic acids, e.g. lactic acid, mandelic acid, succinic acid and itaconic acid are up-and-coming substances used on large scale (Murali et al., 2017; Vijayakumar et al., 2008).

Many carboxylic acids are nowadays produced fermentatively out of carbohydrates (Datta and Henry, 2006). During the fermentation process, the pH has to be controlled to ensure ideal growing conditions and to prevent product inhibition of the bacteria (Halley and Dorgan, 2011; Shen et al., 2010; Stevens, 2012). Conventionally, the pH is maintained by addition of calcium hydroxide or calcium carbonate to the fermentation broth. After the fermentation, sulfuric acid is added to release the carboxylic acid from its salt form, resulting in a stoichiometric production of gypsum as side-product (Datta and Henry, 2006). This method is both costly and undesired for larger scale production, e.g. for acids as monomers for biopolymers (Datta and Henry, 2006; Evangelista and Nikolov, 1996; King, 1992; Straathof, 2011; Wasewar et al., 2004), since gypsum cannot be sold on the market profitable at

much larger than current scales due to an oversupply from other sources (e.g. flue gas scrubbing). Techniques such as reactive distillation (Kumar et al., 2006), stripping (Han and Hong, 1996), reactive liquid–liquid extraction (Wasewar et al., 2004), adsorption (Aljundi et al., 2005; Bayazit et al., 2011) and membrane processes (electro-dialysis, ultrafiltration, nanofiltration) (Pal et al., 2009) have been investigated to circumvent continuous broth neutralization and thus gypsum formation (Singhvi et al., 2018).

While conventional liquid–liquid extraction represents a very straight forward approach, small carboxylic acids are due to their hydrophilic nature difficult to extract. However, reactive extraction is highly efficient to extract these carboxylic acids out of dilute aqueous streams ($\ll 10$ wt% carboxylic acid) (Krzyzaniak et al., 2013; López-Garzón and Straathof, 2014). The most promising reactive agents are tertiary amines, such as tri-n-octylamine (TOA) (Choudhury and Swaminathan, 1998; Udachan and Sahoo, 2014).

Although the thermodynamics of the reactive extraction processes have been well studied (Han and Hong, 1996; King, 1992; Krzyzaniak et al., 2014, 2013; Procházka et al., 1994; Qin et al., 2003; Susanti et al., 2016; Tamada et al., 1990), operational limitations such as the formation of stable emulsions and limited flexibility in solvent/feed (S/F) phase ratios remain adversely. However, by applying a membrane supported extraction (MSE), emulsification may be prevented and an (almost) unlimited range

* Corresponding author.

E-mail address: b.schuur@utwente.nl (B. Schuur).

Nomenclature

Abbreviations

CA	Carboxylic acid deprotonated
CAH	Carboxylic acid, protonated
CAHTOA	Carboxylic acid-TOA-complex
LA	Lactic acid
MSRE	Membrane supported reactive extraction
NTS	Number of theoretical stages
S/F	Solvent to Feed ratio
PTFE	Polytetrafluorethylene
TOA	Tri-n-octylamine

Symbols

D	Diffusion coefficient [cm^2/s]
Δ_{mem}	Membrane wall thickness [m]
F	Flow rate [m^3/s]
J	Flux [mol/s]
K	Mass transfer coefficient [m/s]
K	Overall mass transfer coefficient [m/s]
K_a	Phase dissociation equilibrium constant [L/mol]
K_c	Complexation constant [L/mol]
M	Molecular weight [g/mol]
M	Physical distribution coefficient [-]

N	Slice number of membrane contactor [-]
η	Dynamic viscosity [$\text{mPa}\cdot\text{s}$]
τ	Residence time [s]
T	Temperature [K]
V	Volume [m^3]
V_b	Molar volume at normal boiling point [cm^3/mol]
X	Solvent association factor [-]
*	At interface [-]

Subscripts

Aq	Aqueous phase
c	capillary
equil	At equilibrium
F	Feed
I	Inner
init	Initial
l	logarithmic
mem	Membrane
o	outer
ov	Overall
org	Organic phase
s	Shell

of (S/F) becomes accessible (De Sitter et al., 2018; Gössi et al., 2020; Grzenia et al., 2012, 2010).

Membrane supported extractions of carboxylic acids have been reported previously (Gössi et al., 2020; Marták et al., 2008; Schlosser et al., 2005)(De Sitter et al., 2018). While mass transfer dependencies have been investigated experimentally, no mass transfer models have been reported that consider reaction and extraction in parallel. Additionally, publications dealing with membrane supported countercurrent membrane extraction are scarce (Hereijgers et al., 2015; Kołtuniewicz et al., 2012). However, countercurrent extraction maintains the maximum driving force and therefore minimizes the amount of solvent needed while maximizing the extraction efficiency.

We here report a study that explores the use of chemically highly stable PTFE membranes in countercurrent extraction processes. So far, for these types of membranes, only proof of concept has been reported (Gössi et al., 2020). It could be shown that the use of membranes as extraction interface reduces solvent toxicity towards microorganisms. This is crucial for an *in-situ* product removal process.

The membranes used for this work strongly differ from membranes in commercially available membrane contactors in terms of membrane material, pore diameter and wall thickness. Commercially available membrane contactors are often hollow fiber contactors, providing remarkably large relative membrane contact areas (m^2/m^3), but they tend to block due to their dense packing and are therefore not suitable for a process aiming at *in-situ* removal out of fermentation broths. We therefore propose the use of capillary contactors. The membrane consists of PTFE while the commercially available membranes are mostly of polypropylene. The membrane thickness of 270 μm is rather high, compared to commercially available membranes with about 40–80 μm wall thickness. The pore diameters are much bigger than usual (0.5 μm instead of $\sim 0.05 \mu\text{m}$). This is beneficial due to the rather high viscosity of the solvent and the diffusion-only mass transfer through the pores. While the use of a hydrophilic membrane would offer the advantage that the pores of the membrane contactor would be filled with the less viscous aqueous phase, the long-

term stability of such coatings is still an issue. Furthermore the pressure control with a hydrophilic membrane is more challenging as we found out ourselves, in agreement with earlier literature (Prasad and Sirkar, 1988; Upadhyaya et al., 2018).

The use of these innovative types of membranes might provide significant improvement regarding process stability and cost-efficiency. This paper describes the development of a countercurrent, multistage extraction process for carboxylic acids using a new type of robust membranes. In order to do so, following information was required: The combination of extractant, diluent and carboxylic acid, the membrane properties, the number of stages required for the process, and finally, the theoretical length for one stage. Because the mass transfer rates for these membranes had not yet been determined for liquid–liquid reactive extraction of carboxylic acids, it was necessary to combine experimental studies on mass transfer with modeling studies to describe the membrane supported countercurrent reactive extraction process.

Thus, we here report experimentally obtained mass transfer coefficients. The mass transfer and reaction in parallel model was applied to fit the appropriate mass transfer coefficient and to develop a model to simulate countercurrent extraction. The model was experimentally validated and then used to calculate the length of membrane modules needed to facilitate up to three theoretical countercurrent extraction stages in a single module, a first in liquid–liquid membrane contactors.

By using chemically resistant PTFE membranes, the operation window of MSRE can be expanded towards a wider range of chemically demanding applications.

2. Experimental section

2.1. Chemicals

All chemicals were purchased from Sigma Aldrich Switzerland. Tri-n-octylamine (TOA) (98 %), sodium hydroxide standard solution (volumetric for titration 0.1 M NaOH), copper(II) sulfate (>99 %), 1-decanol ($\geq 98 \%$), 1-octanol (>99 %) itaconic acid (>99 %), mandelic acid (99 %), citric acid ($\geq 99.5 \%$) and succinic acid

(>99 %) were used. The aqueous lactic acid solutions were prepared using 80 wt% lactic acid.

2.2. Experimental setup

A membrane extraction setup consisting of two 2 L vessels and two gear pumps as shown in Fig. 1 was used. Needle valves were used to adjust the pressure on both phases. Temperature, flow rates, density (E + H Cubemass DCI) and pressure were recorded.

Phase equilibrium experiments were performed in 50 mL Falcon tubes. An Agilent 62545A hybridization oven was used for shaking and temperature control. An Eppendorf Centrifuge 5804 R, A-4-44 Rotor, at 5000 RPM (~4500 g) was used to reach phase separation after extraction, since the solvent–water systems that were investigated tend to form stable emulsions.

2.3. Analytical techniques

The analysis of the carboxylic acid concentration in the aqueous phase was performed either by titration or by HPLC, the total organic phase concentration was determined by mass balance. A Mettler Toledo G20 device was used for the potentiometric direct titration method (0.1 M NaOH). The HPLC was equipped with Agilent Hi-Plex H, 7.7×300 mm, $8 \mu\text{m}$ column and a RI Detector. The mobile phase was 5 mM sulfuric acid solution with an isocratic flow rate of 0.6 mL/min and an oven temperature of 65 °C. The retention time for lactic acid was 6.3–6.7 min with a total runtime of 10 min. If not stated differently, all measurements were performed in triplicates. The error was below 3% for both methods.

Viscosity measurements were done using a Haake RheoStress 1 viscosimeter from Thermo Scientific, with a Rotor Z34 DIN 53,019 Serie 1.

2.4. Experimental methods

2.4.1. Complexation constant trials

Phase equilibrium trials were performed to determine the complexation constants K_c of different carboxylic acids with TOA. Aliquots of 1–35 mL of an aqueous stock solution containing 0.12 wt% of carboxylic acid were extracted with 1 mL of 20 wt% TOA in 1-octanol or 1-decanol for 3 h at 25 °C under stirring. The concentration of the remaining carboxylic acid in the aqueous

phase was measured using HPLC after centrifugation. The concentration of the carboxylic acid bound to the reactive agent in the organic phase was determined by mass balance, similar to the procedure reported by (Krzyzaniak et al., 2014).

2.4.2. Membrane supported extraction experiments

All MSRE experiments were started by circulating the aqueous phase with an overpressure of about 60–100 mbar to ambient pressure. Afterwards, the circulation of the organic phase was started, keeping the pressure about 50 mbar lower than the aqueous phase. This avoids breakthrough of organic phase into the aqueous phase.

The organic phase was pumped through the lumen side of the hydrophobic capillaries and the aqueous phase through the shell side of the membrane contactor to maximize the contact area. All experiments were performed at 25 °C.

Two different (hydrophobic) PTFE membranes were tested. Their properties are listed in Table 1.

All membrane modules were built using these PTFE membranes. Table 2 lists the modules built:

Since only small-sized membrane modules were used, both the aqueous and the organic phase were circulated until reaching equilibrium, except for the results in section 4.3, which are once-through experiments. The membrane circulation experiments were performed in co-current mode. However, due to the short length of the membrane contactor, no influence was observed on the mass transfer results.

Membrane supported reactive extractions were performed with 0.1 M carboxylic acid as aqueous phase, which is a realistic concentration for an *in-situ* extraction process out of fermentation broths (Gössi et al., 2020). A starting pH of < 2 was measured for all MSRE experiments, indicating a full protonation of the carboxylic acid (all $\text{p}K_a > 3.1$).

2.5. Numerical methods

Model equations were solved using MATLAB version R2019b.

For the equilibrium model, lsqnonlin solver was used to fit the complexation constant $K_{c,\text{org}}$ to experimental data. All other concentrations in this stage were calculated using known equilibria constants (dissociation equilibrium K_a , and physical distribution coefficient m) and the parameter to fit, $K_{c,\text{org}}$. For simulations of

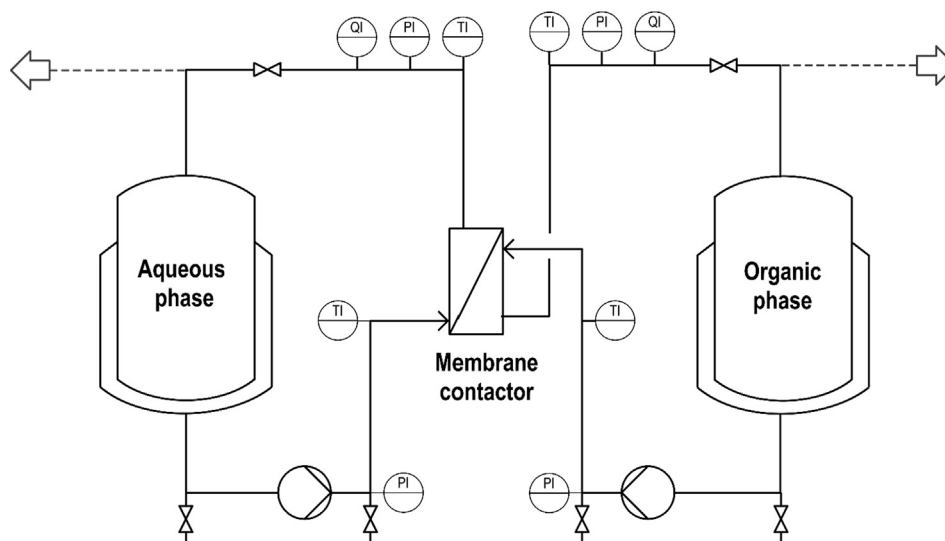


Fig. 1. MSRE-Setup, gear pumps range 5 L/h – 60 L/h, temperature can be adjusted between 10 and 60 °C, all phase-contacting parts are made from PVDF, PTFE, glass, or stainless steel (1.4404). Dotted green lines represent once-through experiments where no circulation was applied.

Table 1
Membranes used for this work.

Membrane No.	Membrane Material	Porosity [%]	Pore diameter [μm]	Inner diameter [mm]	Outer diameter [mm]	Wall thickness [μm]
1	PTFE	54	0.47	2.97	3.49	260
2	PTFE	40*	0.50*	2.95*	3.11*	80*

* Based on Field Emission Scanning Electron Microscopy (FESEM). Based on the FESEM observations, the tortuosity τ was estimated to be 2.5, which is in good agreement with published tortuosity's of stretched PTFE membranes (Cramer et al., 2021). Both membranes were purchased from Memo3 GmbH, Switzerland. A FESEM image of membrane 1 is shown in Fig. 3 and in the Appendix. Data not marked with an * were given by the manufacturer.

Table 2
Membrane contactors built for this work.

Contactor No.	Membrane No. (from Table 1)	Number of Fibers [-]	Inner Diameter shell side [cm]	Length [cm]	Contact Area [m ²]
1	1	7	2.5	7.7	0.0050
2	2	7	2.5	7.7	0.0043
3	1	7	2.5	77	0.059
4	1	1	0.8	500	0.055
5	1	1	0.8	700	0.077
6*	1	1	0.8	1200	0.132

* Module 6 was created by linking module 4 and 5 together.

multi equilibrium stage processes, the fitted $K_{c,org}$ was used together with K_a and m and other process parameters such as flow rates to calculate the concentrations in both phases in each of the stages using the overall mass balance over the process in combination with stage-wise mass balances.

For the kinetic modelling, a membrane module was divided into N slices of each 10 cm length, N being determined by the physical length of the module. The contact area and volume of each slice can be calculated from the module design. Consequently, the residence time in each slice can be calculated using the flow rates. The concentration of bound carboxylic acid in the organic phase influences the viscosity. The diffusion coefficient was calculated for each slice based on a linear interpolation of the viscosity based on two viscosity measurements. The use of a linear dependency by approximation was justified based on a linear fit we made to represent literature data (Zheng et al., 2009) for a similar system in good agreement. The viscosity of unloaded 20 wt% TOA in 1-decanol was measured at 10 mPa*s. After equilibration with an equivalent volume of 7 wt% lactic acid a 1 lactic acid per 1 TOA loading (molar base) resulted and a viscosity of 24 mPa*s was measured.

Based on the concentration gradient between the organic and aqueous slice in contact, the enhancement factor and thereon the mass transfer rate was calculated. Fig. 2 schematically shows the kinetic countercurrent modelling approach:

The resulting mass transfer rates were calculated using the ode113 solver in MATLAB according to the model equations described in Section 3.

3. Theory

A homogenous reaction model according to (Schuur et al., 2008) was used and the complexation constant was calculated as shown in Equation (1).

$$K_{c,org} = \frac{[CAHTOA]_{org}}{[CAH]_{org} \cdot [TOA]_{org}} \quad (1)$$

Additionally, the complexation constants were also calculated for a heterogenous model (Qin et al., 2003).

$$K_c = \frac{[CAHTOA]_{org}}{[CAH]_{aq} \cdot [TOA]_{org}} \quad (2)$$

A previous publication showed that for active diluents such as 1-octanol and 1-decanol a stoichiometry 1:1 between acid and base is expected, as shown by (Sprakel and Schuur, 2019). Therefore, in this work we have also taken a 1:1 stoichiometry in all cal-

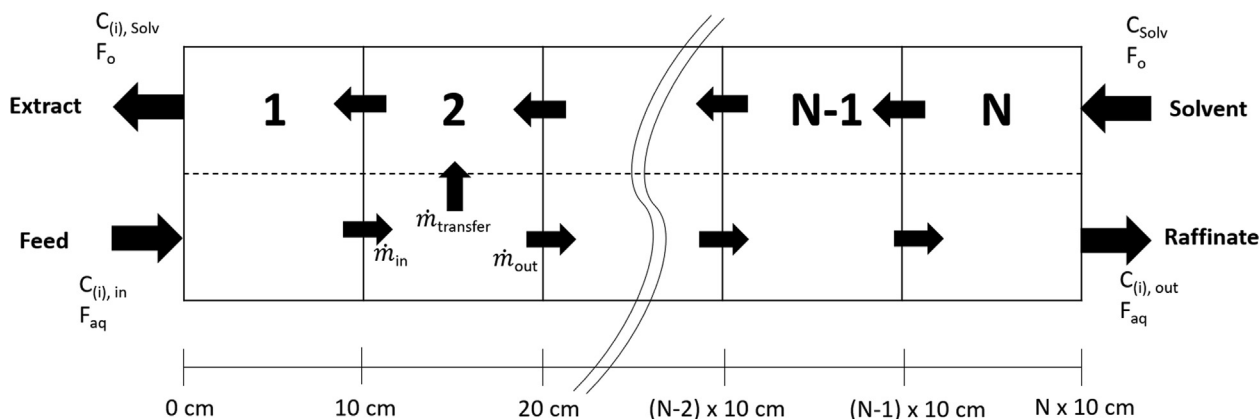


Fig. 2. Countercurrent extraction model based on mass transfer and parallel reaction, $C_{(i)}$ = concentration of carboxylic acid. F_o and F_{aq} = flow rates of organic and aqueous phase, N = slice number. Constant volumes were assumed.

culations. Physical partitioning coefficients for 1-octanol were taken from literature and measured for 1-decanol, respectively (GESTIS, accessed 2021).

A detailed description about the equilibrium modelling can be found in the Appendix.

Fig. 3 shows a schematic depiction of a concentration profile over a membrane. The hydrophobic membrane is filled with the organic solvent.

In a dynamic system like in MSRE, not only the equilibria are of relevance, but also flux equations.

Thus, a kinetic model was developed, involving the overall mass transfer coefficient K_{ov} as given in Equation (3) (Riedl, 2021; Riedl et al., 2011).

$$\frac{dn_{CAH, aq}}{dt} = -K_{ov} \cdot A \cdot \left([CAH]_{aq} - \frac{[CAH]_{org}}{m} \right) \quad (3)$$

In Equation (3), A stands for the contact area available for the mass transfer (in m^2) and m as the physical distribution coefficient. The carboxylic acid flux from the aqueous phase to the organic phase can be described as a series of three individual mass transfer coefficients. Equation (4) shows the correlation for a reactive extraction using a hydrophobic membrane with the organic phase in the capillaries.

$$\frac{1}{K_{ov}} = \frac{1}{k_{ov} \cdot A_o} = \frac{1}{E_{A, aq} \cdot k_s \cdot A_o} + \frac{m}{E_{A, org} \cdot k_{mem} \cdot A_{lm}} + \frac{m}{E_{A, org} \cdot k_c \cdot A_i} \quad (4)$$

with the mass transfer coefficient in the aqueous concentration boundary layer k_s , the mass transfer coefficient through the membrane pores k_{mem} and the mass transfer coefficient through the organic boundary layer k_c (Crespo et al., 2000), all three of them being the ratio of the diffusivity over the thickness of the respective layer. A_i , A_{lm} and A_o stand for the contact areas calculated for the inner, logarithmic mean, and outer diameter of the fibers, respectively. E_A stands for the enhancement factor in the aqueous and organic phase (Equation (5)).

In Equation (4), mass transfer resistances in the boundary layers on the aqueous side of the membrane, and on the organic side of the membrane are included. By increasing the flow rates in the aqueous phase, the overall mass transfer coefficient K_{ov} should increase if there is significant mass transfer resistance in the aqueous boundary layer. The same applies for the organic phase if the mass transfer resistance is in this phase. In cases where the overall rate is independent of either one or both boundary layers, Equation (3) simplifies. The overall mass transfer coefficient K_{ov} can be used to predict the mass transfer in membrane supported liquid–liquid extraction.

E_A in Equation (5) stands for the enhancement factor which must be considered for any liquid–liquid reactive extractions, since –compared with just a physical extraction– the process can be enhanced, depending on the relative rate of the reaction(s) with respect to the mass transfer rate(s), and thus be more efficient. This enhancement can be described as a ratio between the mass transfer with a chemical reaction in relation to the mass transfer by physical extraction only (i.e. without extractant) (Westerterp et al., 1991).

$$E_A = \frac{J_{CAH, chem}}{J_{CAH, phys}} \quad (5)$$

An important note regarding the E_A in Equation (4) is that we include this in all terms of the Equation since both in the aqueous phase and in the organic phase reactions occur, as follows from Fig. 3. In the aqueous phase it is the dissociation reaction, and in the organic phase the complexation reaction. For any reaction, the Hatta number can be used to determine whether a reaction is slow or fast compared to mass transfer. For very slow reactions compared to mass transfer, the overall rate is only determined by the reaction kinetics and the enhancement factor is then equal unity. In case of a fast reaction compared to mass transfer, the enhancement factor is larger than unity (Westerterp et al., 1991). For a homogeneous organic phase reaction between a carboxylic acid (CAH) and tri-*n*-octylamine (TOA) of order p and q , the Hatta number is defined as:

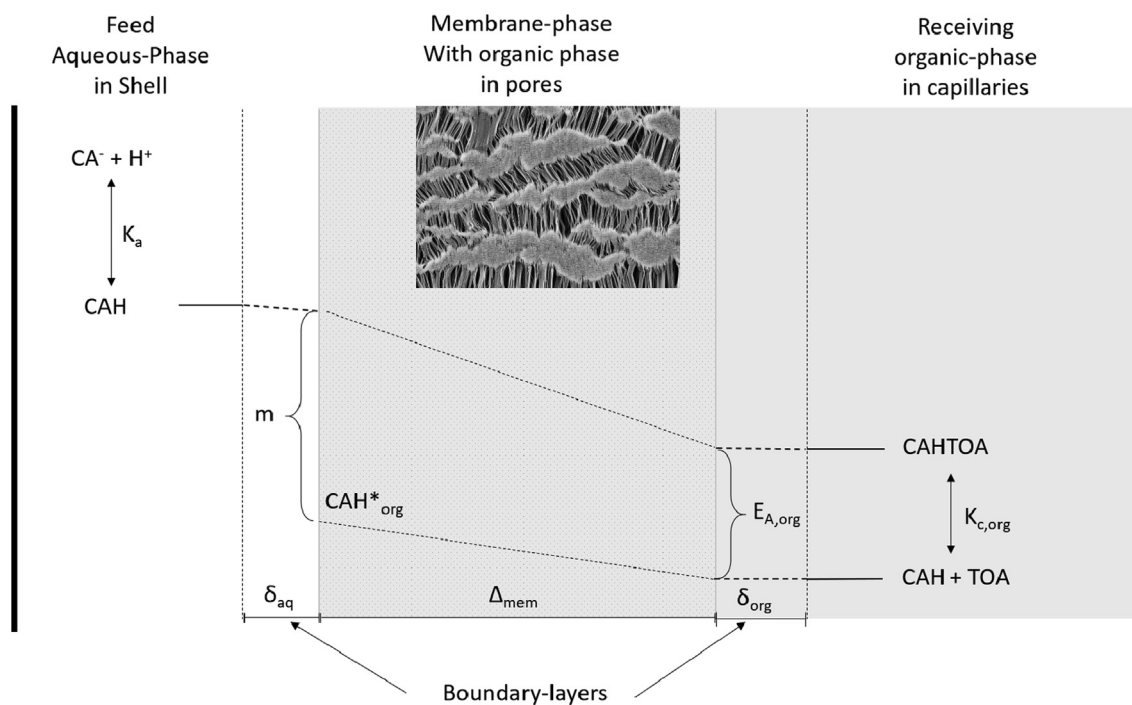


Fig. 3. Schematic representation of the concentration profile over a (porous) membrane. CAH = protonated carboxylic acid, CAH* = concentration at the interface, TOA = tri-*n*-octylamine (diluted in 1-octanol or 1-decanol), CAHTOA = carboxylic acid-TOA complex, m = physical distribution coefficient, E_A = Enhancement factor, K_a = Acid dissociation constant, $K_{c, org}$ = homogenous complexation constant. The membrane phase contains an electron microscopy image of membrane 2.

$$Ha_{CAH+TOA} = \frac{\sqrt{\frac{2}{p+1} D_{CA} k_{pq} [CAH^*]_{org}^{p-1} [TOA]_{org}^q}}{k_{L,org}} \quad (6)$$

in which $[CAH^*]$ stands for the concentration at the organic side of the interface. This can be calculated by multiplying the physical distribution coefficient m with the interfacial concentration on the aqueous phase $[CAH^*]_{aq}$.

With p and $q = 1$, typical for acid extractions with active, hydrogen bonding diluents such as 1-octanol and 1-decanol, especially for relatively low acid concentrations (Sprakel and Schuur, 2019), the Equation simplifies to:

$$Ha_{CAH+TOA} = \frac{\sqrt{D_{CA} k_{pq} [TOA]_{org}}}{k_{CA,org}} \quad (7)$$

For very slow reactions compared to mass transfer, Ha is < 0.2 . For medium reaction rates $0.2 < Ha < 2$. In case of $2 < Ha \ll E_{A\infty}$, the reaction is fast and in case of $Ha > E_{A\infty}$, the reaction is instantaneous (Westerterp et al., 1991). A recent publication found reaction rates of $0.332\text{--}0.430 \text{ m}^3/\text{mol}\cdot\text{s}$ for the reactive extraction of propionic and malic acid using trioctylamine in 1-decanol (Inyang and Lokhat, 2020), resulting in $Ha \geq 1000 > E_{A\infty}$. Therefore $E_{A\infty}$ was used as enhancement factor, for which Equation (8) applies to instantaneous equilibrium reactions (Ferreira et al., 2005; Westerterp et al., 1991).

$$E_{A\infty,org} = 1 + \frac{D_{CA}}{D_{CAHTOA}} \frac{K_{c,org} [TOA]_{org}}{1 + \frac{D_{CAHTOA}}{D_{TOA}} K_{c,org} [CAH^*]_{org}} \quad (8)$$

The enhancement factor in the aqueous phase can be interpreted as the possibility of replenishing depleted CAH due to transfer by protonation of CA^- . At any position in the aqueous film layer, CA^- may be instantaneously converted into CAH, and therefore the $E_{A\infty,aq}$ is defined as the ratio of total available carboxylic acid in all forms (protonated and deprotonated) to CAH. And thus:

$$E_{A\infty,aq} = 1 + \frac{K_a}{H^+} \quad (9)$$

The diffusion coefficients in Equation (8) were calculated using Wilke-Chang Equation (see Appendix A8)

Reports on the determination of mass transfer rates in membrane contactors are rather scarce (Lightfoot, 1996; Nunes and Peinemann, 2006; Patil et al., 2017; Riedl et al., 2011; Riedl and Raiser, 2008). Since a new type of membrane was used for this work, the determination of mass transfer rates is crucial for future process development considerations. Knowing the mass transfer resistance, the mass transfer rates can often be improved by using optimized flow conditions (Kiani et al., 1986; Prasad et al., 1986).

4. Results and discussion

4.1. Complexation constant K_c

The experimentally determined total aqueous concentrations of carboxylic acid $[CA^-]_{aq} + [CAH]_{aq}$ in equilibrium extraction experiments were used to fit K_c using Equations (1) and (2) (see Appendix A1–A7). Fig. 4 shows the compliance between the fitted model and experimental values for lactic acid.

The found complexation constants for several acids with their accuracy are given in Table 3.

Publications working with TOA/ 1-octanol led to a complexation constant K_c of 200 L/mol for lactic acid and 119 L/mol for succinic acid (Qin et al., 2003; Zhou et al., 2013), working with a S/F of 1 and variable lactic acid concentrations. Using another popular tertiary amine, Alamine 336 in 1-octanol, a complexation constant K_c of 75 L/mol has been reported for the 1:1 complex of lactic acid and

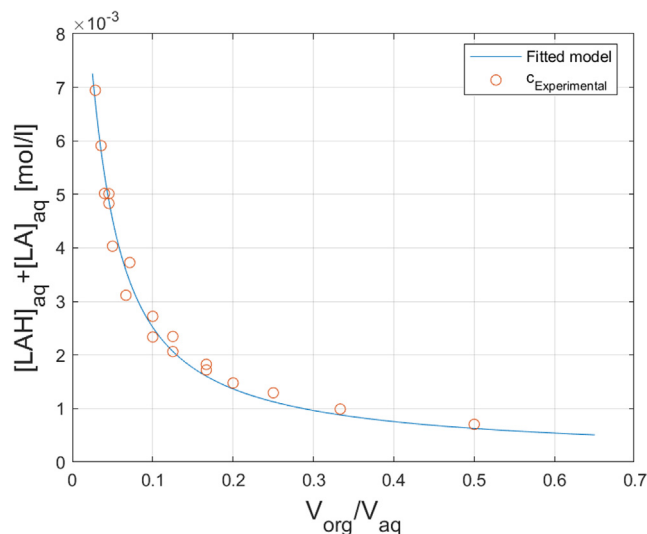


Fig. 4. Reactive extraction model to determine complexation constant K_c for lactic acid. Initial lactic acid concentration of 0.013 M (0.12 wt%), a TOA concentration of 0.56 M (20 wt%) in 1-octanol and a range of V_{org}/V_{aq} between 0.03 and 0.50.

11 L/mol for the 2:1 complex (Wasewar et al., 2004, 2003). It can thus be concluded that our results are in line with previously reported values. Furthermore, comparing 1-decanol results with 1-octanol results, it follows that the complexation is favored by the shorter alcohol, which is a logical result of having a higher concentration of OH-functional groups per kg diluent present. The OH-groups stabilize the complexes between TOA and CAH.

4.2. Membrane recirculation extraction

The MSRE set-up described in section 2.2 was used for all membrane experiments. Samples were analyzed according to section 2.3. If not stated differently, the experiments were performed at 25 °C, with 20 wt% TOA in 1-octanol or 1-decanol.

Both membranes tested are non-selective, meaning that they do not influence the phase equilibrium in any way. All distribution coefficients obtained from MSRE were in excellent accordance with the batch test distribution coefficients.

MSRE experiments were performed using different flow rates from 6 to 50 kg/h on the organic and aqueous phase, respectively, using contactor 3 from Table 2.

Fig. 5 shows the concentration profile of three experiments with different flow rates and initially 3 wt% lactic acid in the aqueous phase. From Fig. 5 it follows that the concentration profiles in all experiments are very similar and are thus not affected by either an increased aqueous phase flowrate or an organic phase flowrate.

The resulting mass transfer coefficients were calculated using Equation (3). During all experiments, the overall mass transfer coefficients K_{ov} remained constant at $2.2 \cdot 10^{-7} \text{ m/s}$ within the confidence of 10%. This leads to the conclusion that the mass transfer resistance is mainly inside the membrane. Previous studies for the MSRE of carboxylic acids with amines have identified the aqueous phase (De Sitter et al., 2018) or the membrane phase (Grzenia et al., 2012, 2010; Juang and Huang, 1997) as limiting. However, these publications worked with polypropylene or PVDF membranes with variant membrane thicknesses.

Knowing that the mass transfer resistance is in the membrane phase, we can now calculate the overall mass transfer coefficient considering only k_{mem} , which can be calculated as follows (Keurentjes et al., 1996):

$$k_{mem} = \frac{\varepsilon D_{S,CAH}}{\tau \Delta_{mem}} \quad (10)$$

Table 3
Complexation constants for different carboxylic acids including standard deviations.

Solvent	1-Octanol			1-Decanol		
	$^{10}\log m^*$ [-]	K_c [L/mol]	$K_{c, org}$ [L/mol]	$^{10}\log m^*$ [-]	K_c [L/mol]	$K_{c, org}$ [L/mol]
Lactic acid	-0.72	120 ± 25	566 ± 25	-0.74	65 ± 9	358 ± 50
Mandelic acid	0.62	1860 ± 288	482 ± 69	0.32	846 ± 283	405 ± 135
Itaconic acid	-0.41	574 ± 22	1383 ± 85	-0.42	380 ± 30	1500 ± 80
Succinic acid	-0.59	84 ± 15	330 ± 50	-0.80	84 ± 4	430 ± 30
Citric acid	-1.57	392 ± 83	14 490 ± 3100	-1.61	305 ± 70	12 361 ± 2868

* Physical partitioning coefficient.

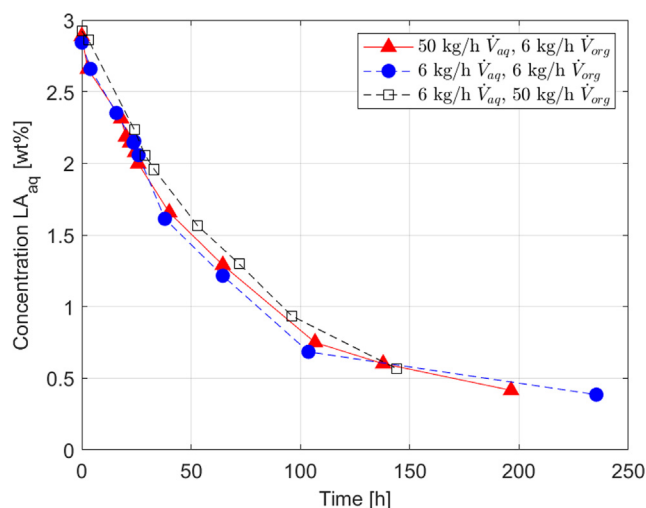


Fig. 5. Membrane supported extraction of lactic acid with different flow rates. 20 wt% TOA in 1-decanol, $V_{org} = 0.6$ L, $V_{aq} = 0.7$ L, $A = 0.059$ m², $LA_{initial} = 2.8$ wt%.

Since the mass transfer coefficient of the membrane phase- which is filled with organic phase- is representing the physical mass transfer only, the enhancement factor in the organic phase (Equation (8)) needs to be considered for reactive extractions.

The mass transfer coefficient k_{mem} depends on the diffusion coefficient and the overall mass transfer coefficient K_{ov} depends on the partition coefficient m and $E_{A,org}$. Therefore, the mass transfer coefficients are different for each of the carboxylic acids investigated. However, an increased physical distribution coefficient m leads to a decreased enhancement factor $E_{A,org}$, strongly reducing the influence on that term in Equation (4). And, despite the difference in molecular size (from 90 g/mol for lactic acid to 192 g/mol for citric acid), the membrane mass transfer coefficient only varies by 10%. Based on empirical equations the mass transfer coefficients k_{aq} and k_{org} are a factor 30 and 1000 times larger than k_{mem} (Viegas et al., 1998), which is well in accordance with our observations for lactic acid, and we can therefore confidently assume that the location of the mass transfer resistance is not changing with other carboxylic acids.

Using the complexation constants, the countercurrent extraction can now be modeled for all carboxylic acids presented in section 4.1. The following section presents the experimental validation and discussion of the model on the example of lactic acid.

4.3. Countercurrent extraction

While membrane recirculation extractions are beneficial for mass transfer investigations with limited contact areas available, a continuous countercurrent process is required for multi-stage

extraction. The results in this section were derived from “once-through” continuous extraction experiments, in which the phases were countercurrently fed. For that purpose, membrane contactors 4, 5 and 6 of Table 2 were used. Flow rates of 1 g/min and 2.5 g/min were used for the organic and aqueous phase, respectively. Four times the residence time ($\tau = 43, 60, 103$ min) were waited before taking samples.

Knowing that the mass transfer resistance lies in the membrane phase, a simple model was developed in MATLAB (Fig. 2) in which only the mass transfer coefficient in the membrane phase was considered. Consequently, only the enhancement factor in the organic phase was applied, and with this model, simulations were run in which the membrane contactor was sliced into compartments to predict the countercurrent extraction, and compare the model with experimental results. A sensitivity investigation proved that discretization into 10 cm compartments is sufficient, as variations in slice thickness up to 20 cm did not impact on the simulation results. Fig. 6 shows the result from these experiments and the model-based predictions, without any fitting required.

Fig. 6 shows, that the predicted concentrations at the contactor exits are in good accordance with the measured values and confirms that only the mass transfer coefficient in the membrane phase (k_{mem}) needs to be considered. A similar model validation for citric acid can be found in the Appendix (Fig. A10). In the case of citric acid, the model shows a small overprediction of only a few percent, which might be explained due to remaining air bubbles reducing the contact area in the module. Having validated a good

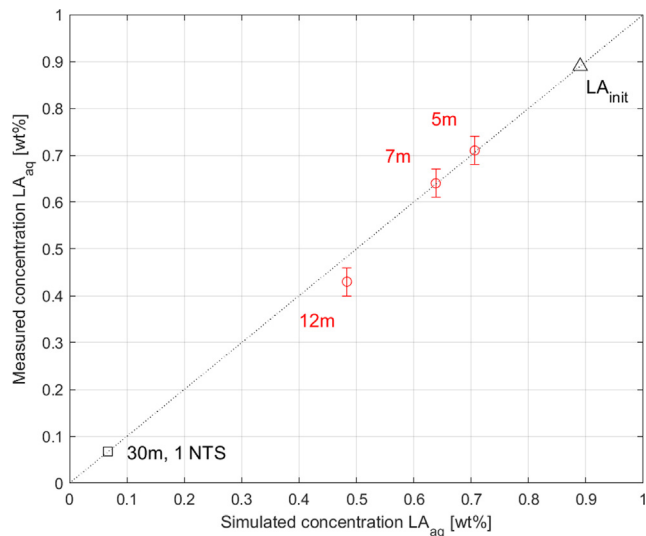


Fig. 6. Countercurrent extraction model validation with experiments using module lengths of 5-, 7- and 12-meter. Also displayed is the prediction of a single equilibrium extraction stage. Extraction of lactic acid, $c_{init} = 0.9$ wt%, 20 wt% TOA in 1-decanol, $V_{org} = 1$ g/min, $V_{aq} = 2.5$ g/min, error bars depicting ± 6% analytical deviation are shown.

agreement between experimental and simulated concentrations, more detailed examination of simulation results was performed.

For that, a 35 m long module was simulated which is (except for the length) identical to contactor 4 of Table 2. Fig. 7 shows the (purely) simulated concentrations and the mass flux over the membrane contactor length. Fig. 7 illustrates that the highest mass transfer rates are at the aqueous entry side of the membrane contactor where the concentration of lactic acid is highest. However, the reduction in the mass transfer rate is not as steep as the reduction in the concentration over the length of the module, which indicates that mass transfer enhancement by the reaction with TOA is important in the modeling of the overall mass transfer.

Fig. 8 shows the simulated profile of $E_{A,org}$ and overall mass transfer coefficient over the same membrane contactor. In accordance with Equation (8), the enhancement factor $E_{A,org}$ strongly influences the overall mass transfer coefficient. Additionally, the overall mass transfer coefficient increases due to the decreasing viscosity from left to right. Significant is that enhancement factor and overall mass transfer coefficient significantly increase from left to right, which confirms the previous conclusion based on the results in Fig. 7, that the mass flux decreases, but not as steep as the concentration gradients.

Based on these results, however, it is concluded that under these conditions the “single-membrane module” contactor with its length of 12 m is not long enough to realize one theoretical extraction step. Fig. 9 shows the predicted concentration profiles for the one-, two- and three-stage countercurrent equilibrium extraction of lactic acid for a 30 m, 50 m and a 66 m long module. The difference in the three lines come from the simultaneous loading of the organic phase with lactic acid, reducing the driving force and leading to higher LA_{aq} concentrations at the same length.

Depending on the flow rate and fiber thickness, a 66 m long module can result in a significant pressure loss over the module. In countercurrent, the pressure loss of the two phases are in the opposite direction, which can lead to a phase breakthrough. Both membranes used can endure an overpressure of 300–400 mbar before a breakthrough of the aqueous phase occurs. An overpressure of at least 50 mbar is required to avoid a breakthrough of organic phase. Nevertheless, by introducing buffer tanks with a pump and a pressure control, no length limitations result.

However, shorter membrane lengths are desirable regarding investment and life cycle costs. The membrane used so far proved

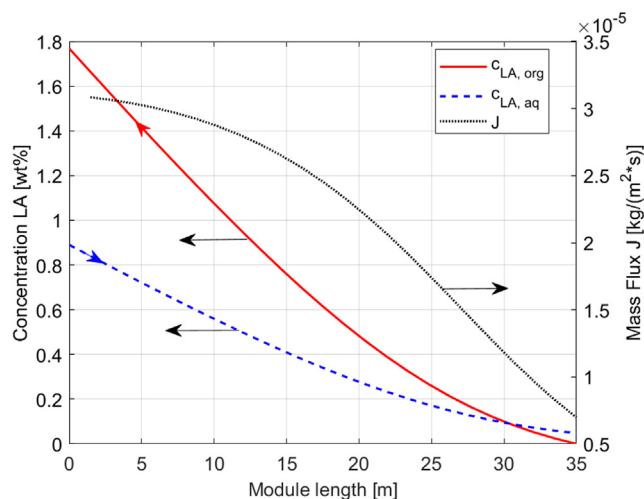


Fig. 7. Simulated lactic acid concentrations and mass flux over membrane contactor length. 20 wt% of TOA in 1-decanol, extraction of lactic acid, $c_{init} = 0.9$ -wt%, $\dot{V}_{org} = 1$ g/min, $\dot{V}_{aq} = 2.5$ g/min.

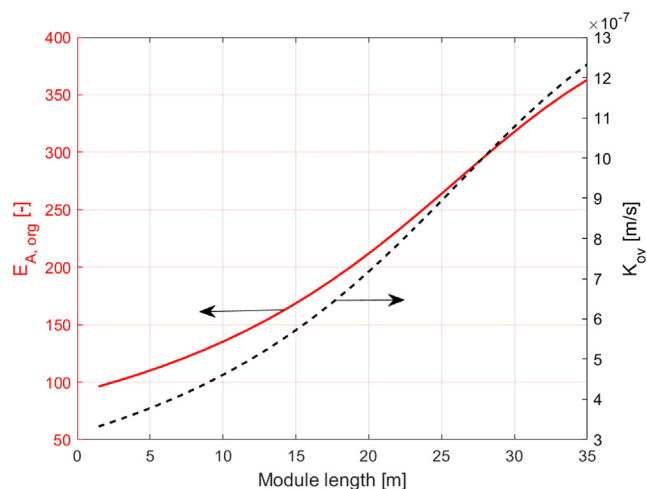


Fig. 8. Enhancement factor and overall mass transfer coefficient over a 35 m membrane contactor. Identical process conditions as in Fig. 7.

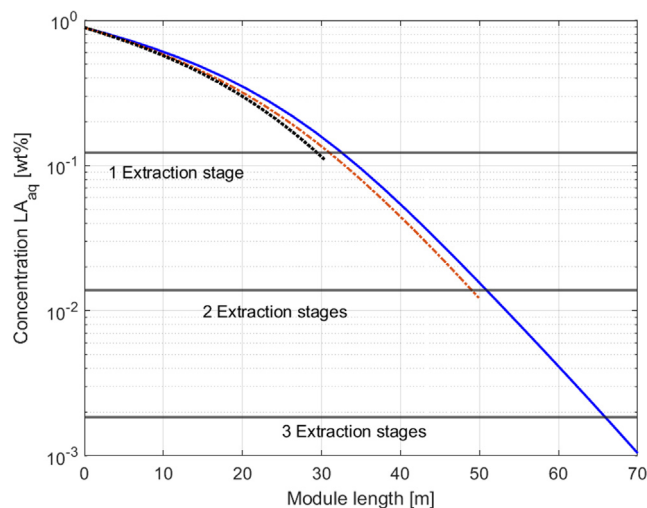


Fig. 9. Countercurrent prediction for one-, two- and three-counter-current equilibrium extraction stages (horizontal black lines indicate raffinate concentrations corresponding to the countercurrent equilibrium stages), $\dot{V}_{org} = 1$ g/min, $\dot{V}_{aq} = 2.5$ g/min, lactic acid $c_{init} = 0.9$ wt%, 20 wt% TOA in 1-decanol.

to represent the major mass transfer resistance. Thus, the thinner PTFE membrane (contactor 2 in Table 2) was tested under the same process conditions. The membranes slightly differ in porosity, but significantly regarding the wall thickness. Flow rate variations were investigated (again 6–50 kg/h for both phases), resulting in no mass transfer increase, stating that still the mass transfer resistance lies in the membrane phase. However, a significant increase in the overall mass transfer coefficient K_{ov} from $2.2 \pm 0.3 \cdot 10^{-7}$ to $4.0 \pm 0.4 \cdot 10^{-7}$ m/s resulted for an extraction with LA_{init} of 1% and 20 wt% TOA in 1-octanol. Thus, the length for a theoretical extraction stage could be reduced from 30 m down to 18 m. This increase in the overall mass transfer coefficient is in good agreement with the predicted increase using Equation (10), which would predict an increase to $4.5 \cdot 10^{-7}$ m/s.

Finally, with the good agreement between experiments and simulations, the required membrane contactor lengths for single, two and three theoretical countercurrent stages extraction were calculated as shown in Table 4.

Table 4Required membrane contactor lengths to reach 1,2 or 3 theoretical countercurrent stages for membrane 1 and 2 with $c_{\text{init}} = 0.1 \text{ M}$, 20 wt% TOA, $\dot{V}_{\text{org}} = 1 \text{ g/min}$, $\dot{V}_{\text{aq}} = 2.5 \text{ g/min}$.

	Carboxylic acid	1-Octanol			1-Decanol		
		NTS 1	NTS 2	NTS 3	NTS 1	NTS 2	NTS 3
Membrane 1 (260 μm wall thickness, see Table 1 for all properties)	Lactic acid	27	45	60	30	50	66
	Mandelic acid	20	40	55	23	45	62
	Itaconic acid	25	41	56	25	42	64
	Succinic acid	37	62	84	39	72	95
	Citric acid	33	55	74	34	55	74
Membrane 2 (80 μm wall thickness, see Table 1 for all properties)	Lactic acid	15	30	42	18	40	60
	Mandelic acid	11	20	28	12	22	34
	Itaconic acid	13	25	32	13	22	34
	Succinic acid	19	35	50	20	38	58
	Citric acid	16	31	44	17	32	50

Noteworthy in Table 4 are the relatively small differences between the carboxylic acids despite the significant differences in physical distribution coefficients. While mandelic acid has a physical distribution coefficient in 1-octanol 150 times higher than citric acid, the required length for a single countercurrent equilibrium extraction stage is reduced by only $\sim 40\%$. This effect can be explained by the reduced enhancement factor in a high physical distribution system.

Moving from octanol to decanol reduces the overall distribution into the solvent phase, but the impact on the required length is limited to an average of 10%. Considering the reduced water solubility and toxicity towards microorganisms, it can be concluded that 1-decanol represents the more appropriate diluent.

5. Conclusions and outlook

A reactive extraction model based on different batch extractions of carboxylic acids by the tertiary amine tri-n-octylamine (TOA) was developed and verified on the example of lactic- and citric acid. Membrane supported extraction experiments were carried out to identify optimal process conditions.

To identify the mass transfer resistance of the MSRE extraction process, the aqueous and organic phase flow rates were varied. In any cases, however, the membrane generated the limiting mass transfer resistance as predicted from the mass transfer model.

A detailed examination of the model was performed on the example of lactic acid and showed that membrane lengths of 30, 50 and 66 m would be required for a one-, two or three-stage extraction process with the 260 μm thick membrane. Using the 80 μm thick membrane, a length of 18, 40 and 60 m would be required for a one-, two or three-stage extraction process.

An interesting alternative to the proposed approach might be the use of phosphonium-based ionic liquids (Marták and Schlosser, 2007; Matsumoto et al., 2004; Oliveira et al., 2012; Reyhanitash et al., 2015). Again, the use of a membrane as artificial interface might be strongly beneficial, since it allows big phase ratios, damping the high costs of ionic liquids.

CRedit authorship contribution statement

Angelo Gössi: Conceptualization, Data curation, Investigation, Methodology, Software, Validation, Visualization, Writing – original draft, Writing – review & editing. **Wolfgang Riedl:** Conceptualization, Investigation, Methodology, Resources, Supervision, Writing – review & editing. **Boelo Schuur:** Conceptualization, Investigation, Methodology, Supervision, Writing – review & editing.

Declaration of Competing Interest

The authors declare that they have no known competing financial interests or personal relationships that could have appeared to influence the work reported in this paper.

Acknowledgements

Boelo Schuur would like to acknowledge Dr. ir. Winkelman and Prof.dr.ir. Heeres from University of Groningen for the discussions on the concept of mass transfer enhancement relations in both liquid phases simultaneously. These discussions have helped conceptualizing the enhancement of mass transfer of weak acids from aqueous phases due to instantaneous dissociation equilibrium as presented in this paper.

This research did not receive any specific grant from funding agencies in the public, commercial, or not-for-profit sectors.

Appendix

Fig. A1 shows the biphasic reactive extraction scheme used for this work, which is similar to the scheme originally presented by Schuur et al. for reactive extraction of an amino acid derivative (Schuur et al., 2008).

The values for the aqueous phase dissociation equilibrium K_a were taken from literature (Eyal and Canari, 1995).

$$K_a = \frac{[CA^-][H^+]}{[CAH]} \quad (\text{A1})$$

In an unbuffered system and at very low concentrations where electrolyte activity coefficients do not significantly deviate from unity, $[H^+]$ is equal to $[CA^-]$ and in the limiting regime where electrolyte activity coefficients are assumed close to unity, we can therefore write:

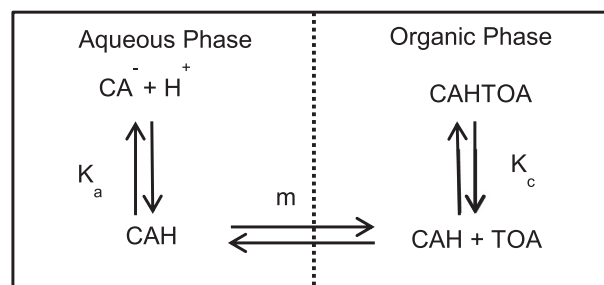


Fig. A1. Single stage reactive extraction system, CA = deprotonated carboxylic acid, CAH = carboxylic acid, TOA = reactive agent (tri-n-octylamine, diluted in 1-octanol or 1-decanol), m = physical distribution coefficient.

$$CAH = \frac{([CA^-])^2}{K_a} \quad (A2)$$

The physical distribution coefficient m at the extraction equilibrium can be calculated according to Equation A(3):

$$m = \frac{[CAH]_{\text{equil.org}}}{[CAH]_{\text{equil.aq}}} \quad (A3)$$

Due to the fact that carboxylic acids have a nonzero solubility in the organic phase and TOA is very hydrophobic, it was assumed that the complexation (from $CAH + TOA$ to $CAHTOA$ in Fig. A1) takes place in the organic phase (Krzyzaniak et al., 2014; Schuur et al., 2008). Since it is difficult to distinguish the very small concentration of unbound carboxylic acid in the organic phase, it is a common approach to describe extraction equilibria of organic acids as an equilibrium spanning both phases, like in Equation A(4) (Bokhove et al., 2012; Han and Hong, 1996; Kertes and King, 1986; Krzyzaniak et al., 2014; Tamada et al., 1990).

$$K_c = \frac{[CAHTOA]_{\text{org}}}{[CAH]_{\text{aq}} \cdot [TOA]_{\text{org}}} \quad (A4)$$

However, when considering dynamic systems with mass transfer and reaction in parallel, it is essential to do include the unbound organic carboxylic acid concentration and the partitioning of the neutral carboxylic acid in the model shown in Fig. A1. The corresponding homogeneous organic phase complexation constant can be calculated according to Equation A(5), which is done in this work.

$$K_{c,org} = \frac{[CAHTOA]_{\text{org}}}{[CAH]_{\text{org}} \cdot [TOA]_{\text{org}}} \quad (A5)$$

The limitation for this approach is that in a reactive system, the partitioning cannot be measured separately from the complexation, and as an approximation, the partition coefficient for reactive systems including amine, and as defined in Equation (3), is determined experimentally for the diluent-only situation and assumed to be similar for the system in which the amine is present in 20 wt%.

Using these Equations, and after fitting the $K_{c,org}$, it is possible to predict the concentration of carboxylic acids in a reactive extraction system for different phase equilibrium experiments.

For the equilibrium model, a total mass balance for a carboxylic acid was used as follows

$$CA_{\text{total}} = V_{\text{aq}} \cdot ([CA^-] + [CAH])_{\text{aq}} + V_{\text{org}} \cdot [CAHTOA]_{\text{org}} \quad (A6)$$

And correspondingly for TOA:

$$TOA_{\text{total}} = V_{\text{org}} \cdot ([TOA] + [CAHTOA])_{\text{org}} \quad (A7)$$

The diffusion coefficients for the solute, extractant and complex were calculated using the Wilke–Chang Equation:

$$D = 7.4 \cdot 10^{-8} \frac{(\chi M)^{0.5} T}{\eta V_b^{0.6}} \quad (A8)$$

In which χ stands for the association factor. The proposed values for water, methanol, ethanol and 1-hexan are 2.6, 1.9, 1.5 and 1, respectively. Thus, $\chi = 2.6$ was chosen for the aqueous phase and $\chi = 1.2$ for the organic phase.

The molecule diameters were calculated according to the method of (Le Bas, 1915) based on their atomic contributions (Henley et al., 2011).

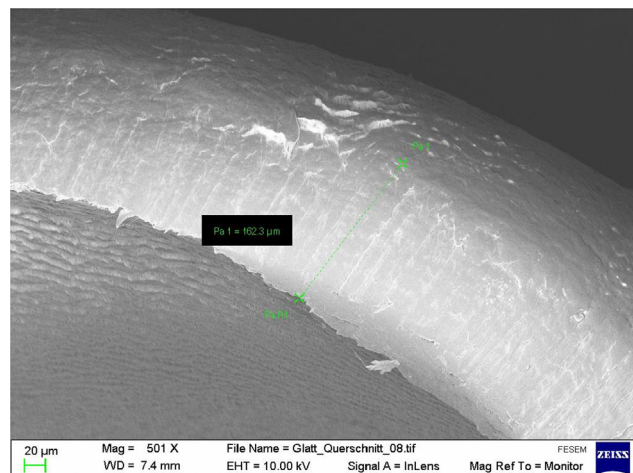


Fig. A9. Cut-through FESEM picture of membrane 1. The straight lines are pores, demonstrating the low tortuosity of the membranes.

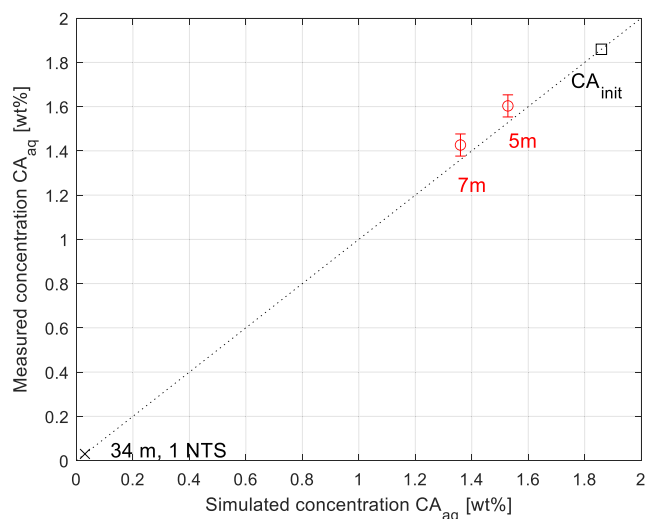


Fig. A10. Countercurrent extraction model validation for citric acid with experiments using module lengths of 5- and 7-meter. Also displayed is the prediction of a single equilibrium extraction stage, $c_{\text{init}} = 1.9$ wt% (0.1 M), 20 wt% TOA in 1-decanol, $V_{\text{org}} = 1$ g/min, $V_{\text{aq}} = 2.5$ g/min, $\pm 5\%$ error bars.

Fig. A9 shows a cut-through FESEM image of membrane 1. The membrane has been stretched for that shot, reducing the wall thickness from 270 μm to 160 μm .

Fig. A10 shows the model validation with citric acid. An excellent agreement between experiment and simulation can be concluded.

References

- Aljundi, I.H., Belovich, J.M., Talu, O., 2005. Adsorption of lactic acid from fermentation broth and aqueous solutions on Zeolite molecular sieves. *Chem. Eng. Sci.* 60 (18), 5004–5009. <https://doi.org/10.1016/j.ces.2005.04.034>.
- Bayazit, S.S., Inci, I., Uslu, H., 2011. Adsorption of lactic acid from model fermentation broth onto activated carbon and amberlite IRA-67. *J. Chem. Eng. Data* 56, 1751–1754. Doi: 10.1021/je1006345.
- Bokhove, J., Schuur, B., de Haan, A.B., 2012. Equilibrium study on the reactive liquid-liquid extraction of 4-cyanopyridine with 4-nonylphenol. *Chem. Eng. Sci.* 82, 215–222. <https://doi.org/10.1016/j.ces.2012.07.038>.
- Choudhury, B., Swaminathan, T., 1998. Lactic acid extraction with trioctyl amine. *Bioprocess Eng.* 19, 317–320. <https://doi.org/10.1007/s004490050526>.

- Straathof, A.J.J., 2011. The Proportion of Downstream Costs in Fermentative Production Processes. *Compr. Biotechnol.* Second Ed. 2, 811–814. <https://doi.org/10.1016/B978-0-08-088504-9.00492-X>.
- Susanti, Winkelman, J.G.M., Schuur, B., Heeres, H.J., Yue, J., 2016. Lactic Acid Extraction and Mass Transfer Characteristics in Slug Flow Capillary Microreactors. *Ind. Eng. Chem. Res.* 55 (16), 4691–4702. <https://doi.org/10.1021/acs.iecr.5b04917>.
- Tamada, J.A., Kertes, A.S., King, C.J., 1990. Extraction of Carboxylic Acids with Amine Extractants. 1. Equilibria and Law of Mass Action Modeling. *Ind. Eng. Chem. Res.* 29 (7), 1319–1326. <https://doi.org/10.1021/ie00103a035>.
- Udachan, I.S., Sahoo, A.K., 2014. A study of parameters affecting the solvent extraction of lactic acid from fermentation broth. *Brazilian J. Chem. Eng.* 31 (3), 821–827. <https://doi.org/10.1590/0104-6632.20140313s00002495>.
- Upadhyaya, L., Qian, X., Ranil Wickramasinghe, S., 2018. Chemical modification of membrane surface – overview. *Curr. Opin. Chem. Eng.* Doi: 10.1016/j.coche.2018.01.002.
- Viegas, R.M.C., Rodríguez, M., Luque, S., Alvarez, J.R., Coelho, I.M., Crespo, J.P.S.G., 1998. Mass transfer correlations in membrane extraction: Analysis of Wilson-plot methodology. *J. Memb. Sci.* 145 (1), 129–142. [https://doi.org/10.1016/S0376-7388\(98\)00074-X](https://doi.org/10.1016/S0376-7388(98)00074-X).
- Vijayakumar, J., Aravindan, R., Viruthagiri, T., 2008. Recent trends in the production, purification and application of lactic acid. *Chem. Biochem. Eng. Q.* 22, 245–264.
- Wasewar, K.L., Pangarkar, V.G., Heesink, A.B.M., Versteeg, G.F., 2003. Intensification of enzymatic conversion of glucose to lactic acid by reactive extraction. *Chem. Eng. Sci.* 58 (15), 3385–3393. [https://doi.org/10.1016/S0009-2509\(03\)00221-5](https://doi.org/10.1016/S0009-2509(03)00221-5).
- Wasewar, K.L., Yawalkar, A.A., Moulijn, J.A., Pangarkar, V.G., 2004. Fermentation of glucose to lactic acid coupled with reactive extraction: A review. *Ind. Eng. Chem. Res.* 43, 5969–5982.
- Westerterp, K.R., Swaaij, V., Beenackers, A.A.C.M., 1991. *Chemical Reactor Design and Operation*.
- Zheng, D., Li, J., Zhou, K., Luo, J. hong, Jin, Y., 2009. Density and Viscosity of Tributyl Phosphate + Kerosene + Phosphoric Acid from (20 to 60) °C. *J. Chem. Eng. Data* 55, 58–61. Doi: 10.1021/JE900559P
- Zhou, Z., Li, Z., Qin, W., 2013. Reactive extraction of saturated aliphatic dicarboxylic acids with trioctylamine in 1-octanol: Equilibria, model, and correlation of apparent reactive equilibrium constants. *Ind. Eng. Chem. Res.* 52 (31), 10795–10801. <https://doi.org/10.1021/ie4008002>.